Finite Element simulations of a phase-field model for mode-III fracture.

by V. Kaushik

1 Motivation

The motivation behind this model is to understand the underlying physics behind branching of cracks during mode-III dynamic failure in glasses through a continuum phase-field model. Further, the model is studied to more importantly analyze the factors affecting the speed of crack growth during Mode-III failure. As a prelimnary excercise a 1-D model is implemented using a staggered formulation to understand the model and the evolution of phase-field variable ϕ(x,t).

2 Phase-field coupled equations

The energy (E) is minimized by taking first variation of it with respect to t and σ and then the coupled differential equations are discretized and implemented.The energy equation for Mode-III dynamic failure is:

$$E = \int [\frac{\rho}{2}(\frac{\partial u}{\partial t})^2 + \frac{\kappa}{2}(\mid \nabla\phi \mid)^2 + hf(\phi) + g(\phi)(\mid \epsilon \mid^2 - \epsilon_c^2)]dxdy \tag{1}$$

where ϕ is the phase field variable such that:
$\phi = 1$ corresponds to unbroken solid; $\phi = 0$ corresponds to a failed material
ϵ_c = critical strain; $\epsilon = \Delta$ u with u(x,y) being a scalar displacement field perpendicular to the x-y plane. $g(\phi)$ is a monotonically increasing function such that g(0) = 0 and g(1) =1. $f(\phi)$ is a double well potential function with minima at $\phi = 0$, 1. By taking first variations of the energy with respect to ϕ and σ :

$$\frac{\partial\phi}{\partial t} = -\chi\frac{\partial E}{\partial\phi} \tag{2}$$

$$\rho\frac{\partial^2 u}{\partial^2 t} = \nabla.\sigma \tag{3}$$

These first variations give rise two interdependent differential equations in ϕ(x,t) and u(x,y).

$$\chi^{-1}\frac{\partial\phi}{\partial t} = \kappa\nabla^2\phi - hf'(\phi) - g'(\phi)(\mid \nabla u \mid^2 - \epsilon_c^2) \tag{4}$$

$$\rho\frac{\partial^2 u}{\partial^2 t} = \mu\nabla.(g(\phi)\nabla u) \tag{5}$$

2.1 The non-dimensionalized variables

Before these equations can be discretized and the equation is non dimensionalized with the non-dimensional controlling parameters. The length is rescaled by ξ, the time with $\frac{\xi}{c}$ and the u(x,y) by $\xi\epsilon_c$. The different non-dimensional parameters consequential in this problem are given in Table. 1.

It has been mentioned that the β and δ are the two controlling parameters with β controlling the inertia with respect to dissipation in the process zone.

Further, δ controls the non-dimensionalized surface energy. Using this non-dimensionalization the coupled PDE's are rewritten:

$$\beta \frac{\partial \hat{\phi}}{\partial \hat{t}} = \hat{\nabla}^2 \hat{\phi} - \delta f'(\hat{\phi}) - g'(\hat{\phi})(\mid \hat{\nabla} \hat{u} \mid^2 - 1) \tag{6}$$

$$\frac{\partial^2 \hat{u}}{\partial^2 \hat{t}} = \hat{\nabla}.(g(\hat{\phi}) \hat{\nabla} \hat{u}) \tag{7}$$

2.2 Finite element discretization and time integration scheme

The coupled equations are discretized as follows for the eqs. 6

$$K^{el}_{ab} = \beta \int_{\Omega} \frac{N^a N^b}{\Delta t} + (1-\theta) \int_{\Omega} \frac{\partial N^a}{\partial \hat{x}} \frac{\partial N^b}{\partial \hat{x}} dv \tag{8}$$

$$R^{el}_a = -\int_{\Omega} \frac{\partial N^a}{\partial \hat{x}} \frac{\partial N^b}{\partial \hat{x}} \hat{phi}^b - \delta f'(\hat{\phi}) - g'(\hat{\phi})(\mid \hat{\nabla} \hat{u} \mid^2 - 1) N^a dv \tag{9}$$

Similarly for the wave equation:

$$M^{el}_{ab} = \int_{\Omega} N^a N^b dv \tag{10}$$

$$R^{el}_a = g(\hat{\phi}) \int_{\Omega} \frac{\partial N^a}{\partial \hat{x}} \frac{\partial N^b}{\partial \hat{x}} dv \tag{11}$$

The wave equation is solved through explicit time integration scheme and the displacements and the velocities are updated using newmark method.

2.3 Time-stepping algorithm

A staggered formulation is implemented with a complete explicit formulation.

- At time $\hat{t}_n$, we are given $\hat{\phi}_n$, $\hat{u}_n$, β and δ.
- Next, Compute the stiffness matrix K^{el}_{ab}, R^{el}_a for the both equations.
- Assemble the Global stiffness and residual matrices
- Solve for $\ddot{\hat{u}}_{n+1}$ and $\hat{\phi}_{n+1}$.
- Update $\dot{\hat{u}}_{n+1}$ and $\hat{u}_{n+1}$ using Newmark scheme.

3 Test cases for the 1-D Phase-field equation

A finite element mesh with 10 elements each of unit length and 11 equally placed nodes is chosen for this study as seen in Fig. 1. All the test cases are studied for $\beta = 1$, and $\delta = 0$.

3.1 Benchmarking

To benchmark the code $g'(\hat{\phi})$ was set to 0 and δ was also set to zero and then the resulting differential equation for ϕ was solved analytically. The analytical solution is :

$$\hat{\phi}(x,t) = \hat{\phi}_0 + \frac{\hat{\phi}_L - \hat{\phi}_0}{L} + \sum_{i=1}^{n} B_n sin(n\pi x/L) e^{-\frac{(n\pi)^2}{L} t}$$

$$BC's\ \hat{\phi}(0,t) = 0$$
$$\hat{\phi}_(L,t) = 1 \tag{12}$$

The FEM solution and the analytical for x = 2, is plotted and compared as seen in the Figs. 2a and b.

Now the second differential equation is benchmarked by choosing $g(\phi) = 1$ as $g'(\hat{\phi})$ was set to 0. We see that the equation reduces to:

$$\frac{\partial^2 \hat{u}}{\partial^2 \hat{t}} = \hat{\nabla}.(\hat{\nabla}\hat{u}) \tag{13}$$

$$\hat{u}(0,t) = 0$$
$$\hat{u}(L,t) = 0$$
$$\hat{u}(L/2,0) = 1 \tag{14}$$

Further analytical solution for this wave equation is obtained:

$$\hat{u}(x,t) = \frac{1}{2}[\sum_{i=1}^{n}[B_n[sin(\frac{n\pi}{L}(x+ct)) + sin(\frac{n\pi}{L}(x+ct))]]] \tag{15}$$

The problem was solved for the same finite element mesh used earlier and the solution is plotted pertaining to x = 5. From the Figs. 3a and b it can be seen that the analytical solution fairly agrees with the FEM solution. It should be noted that to solve the wave equation a viscous constant is added to the residual vector (since the residual is initially zero) and it can be seen clearly that it does have an affect on the solutions. This parameter induces a phase lag in the solution, hence adding levin viscosity for stabilization may not be the best method.

3.2 Test cases to invoke the phase-field and mechanical coupling

Now a test case is simulated to understand the evolution of phase-field variable ϕ by evoking the coupling functions and parameters. The motivation behind the choice of the test case is to show that the variation of $\hat{\phi}$ along x is non-linear, which is an outcome of the coupling. The boundary conditions chosen for this case are as follows:

$$\begin{aligned}\hat{\phi}(0,t) &= 0\\ \hat{\phi}(L,t) &= 1\\ \hat{u}(0,t) &= 0\\ \hat{u}(L,t) &= 0.001\end{aligned} \tag{16}$$

This non-linearity is clearly depicted in the Fig. 4a as $\hat{\phi}$ sluggishly scales with x. Similary, the evolution of $\hat{\phi}$ with time is also plotted as seen in Fig. 4b and the initial instability may pertain to the oscillation of the waves.

A final test case is chosen such that the crack-tip is positioned at x = 1 ($\hat{\phi}$ = 0) i.e, the first element is chosen to have failed. The rest of the elements are initialized to be elastic ($\hat{\phi}$ = 1). A constant velocity of v = 1 units is given to the end of the bar. It can be seen from the Fig. 5 that $\hat{\phi}$ values at x = 3 reduces but then the problem runs into stability issues.

4 Conclusions and Future Work

This preliminary analysis indicates that the 1-D finite element formulation for a this phase-field can only give a brief idea on wether the variation $\hat{\phi}$ with respect to time and space is smooth or not. The differential equation needs to linearized and an implicit formulation needs to be used to circumvent the stability issues. Finally, a 2-D model needs to be implemented to understand the physics behind the zigzag crack-patterning in glasses subjected to mode-III fracture.

5 References

- Unsteady Crack Motion and Branching in a Phase-Field Model of Brittle Fracture, Physical Review Letters, Karma, Alain, Lobkovsky, Alexander E., 2004
- Advanced Engineering Mathematics, 10th Edition, Erwin Kreyszig

Table 1: List of Non-dimensional parameters and the non-dimensionalized variables used.

Variables	$\hat{x} = \mathrm{x}/\xi$	$\hat{t} = \frac{tc}{\xi}$	$\hat{u} = \frac{u}{\xi\epsilon_c}$
Characteristic time	$\tau = \frac{1}{\chi\mu\epsilon_c^2}$		
Shear wave speed	$c = \sqrt{\frac{\mu}{\rho}}$		
Size of the process zone	$\xi = \sqrt{\frac{\kappa}{\mu\epsilon_c^2}}$		
Controlling parameters	$\beta = \frac{c}{\tau\xi}$	$\delta = \frac{h}{\mu\epsilon_c^2}$	
Functions	$f(\phi) = 16\phi^2(1-\phi)^2$	$g(\phi) = 4\phi^3 - 3\phi^4$	

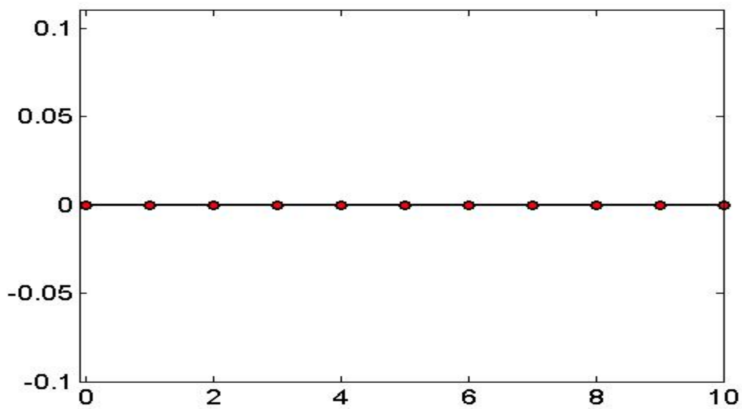

Figure 1: This figure depicts the finite element mesh consisting of 11 nodes with unit spacing and 10 elements. This mesh is used for all the simulations.

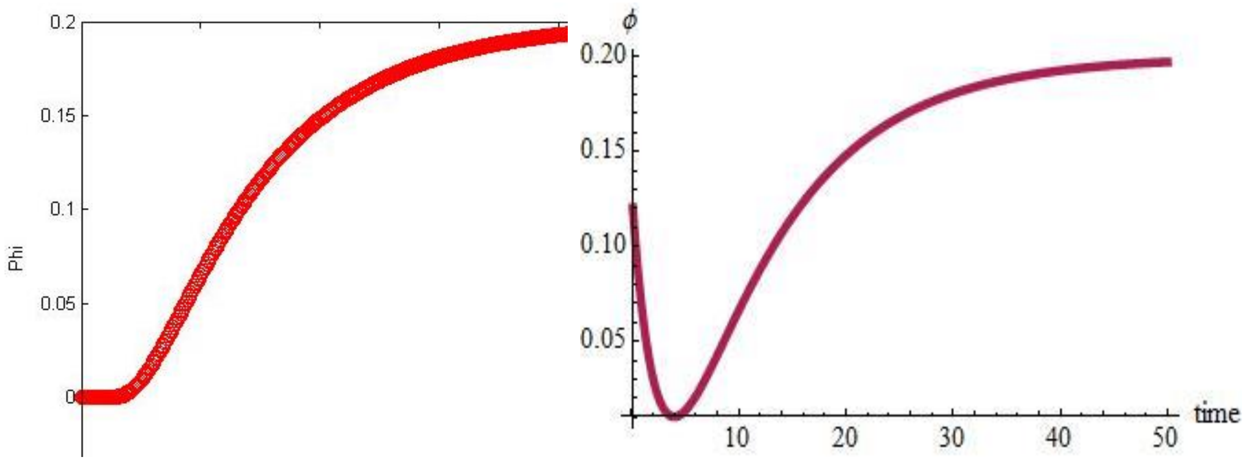

Figure 2a) and b) correspond to the finite element and analytical solutions of the uncoupled differential equation of the phase-field variable Φ at x = 2 for 10 unit long 1D bar element.

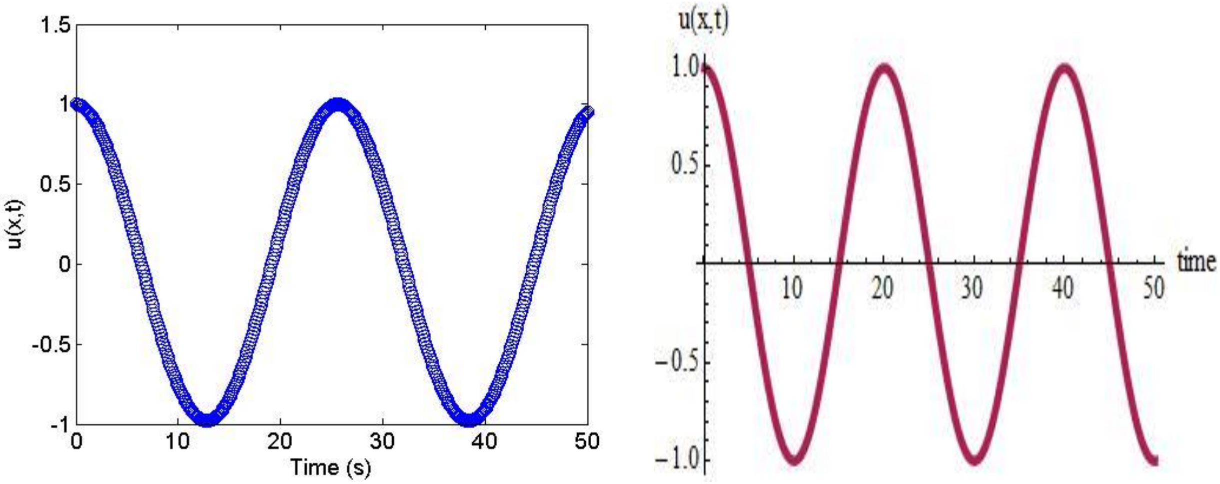

Figure 3a) and b) correspond to the finite element and analytical solutions of the uncoupled differential equation of the scalar-field variable u(x,t) at x = 5 for 10 unit long 1D bar element.

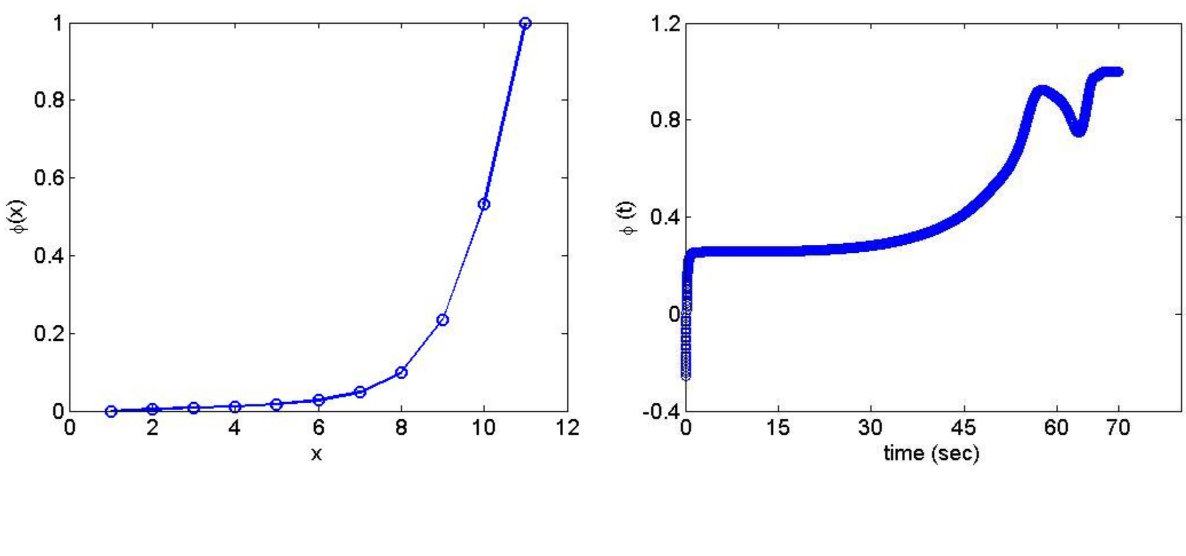

Figure 4a and b correspond to the evolution of Φ(x) and Φ(t) for the third tests case to indicate the non linearity in the evolution of Φ due the mechanical coupling.

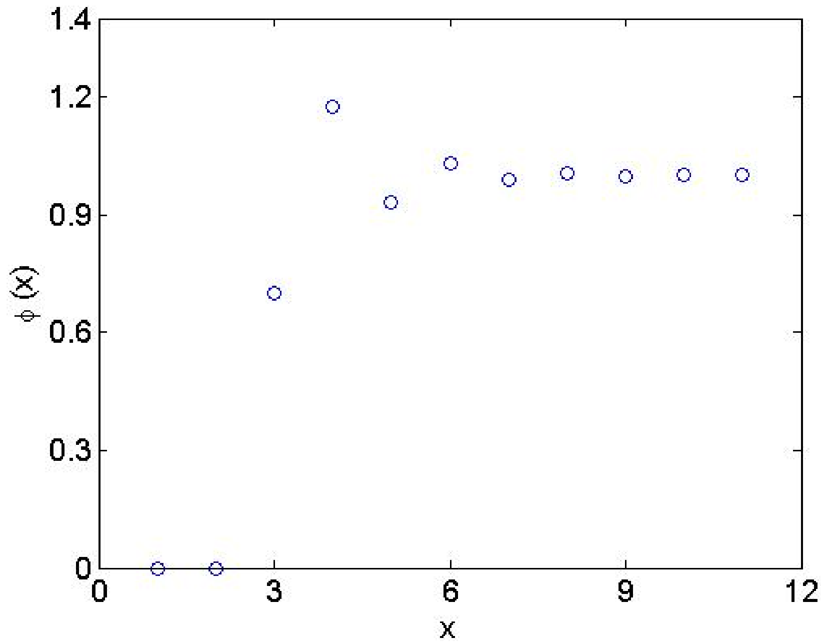

Figure 5 depicts the evolution of Φ with respect to distance for test case-4 where the first element is chosen to have a failed